Unusual thickness dependence of the superconducting transition of α-MoGe thin films

H. Tashiro, J. M. Graybeal, and D. B. Tanner

Department of Physics, University of Florida, Gainesville, Florida 32611, USA

E. J. Nicol

Department of Physics, University of Guelph, Guelph, Ontario, Canada N1G 2W1

J. P. Carbotte

Department of Physics and Astronomy, McMaster University, Hamilton, Ontario, Canada N1G 2W1

G. L. Carr

National Synchrotron Light Source, Brookhaven National Laboratory, Upton, New York 11973, USA

Thin films of α-MoGe show progressively reduced T_c's as the thickness is decreased below 30 nm and the sheet resistance exceeds 100 $\Omega/\square$. We have performed far-infrared transmission and reflection measurements for a set of α-MoGe films to characterize this weakened superconducting state. Our results show the presence of an energy gap with ratio $2\Delta_0/k_B T_c = 3.8 \pm 0.1$ in all films studied, slightly higher than the BCS value, even though the transition temperatures decrease significantly as film thickness is reduced. The material properties follow BCS-Eliashberg theory with a large residual scattering rate but the expected coherence peak seen in the optical scattering rate is lost in the thinner samples. This result cannot be explained within conventional theories.

I. INTRODUCTION

Disorder and reduced dimensionality affect the physical properties of metallic systems in a number of ways. Anomalous diffusion leads to localization of electrons and a related enhancement of the Coulomb interaction via reduced screening,[1,2] seen as an increase in μ^*, the renormalized Coulomb interaction parameter. In a system of lower dimensions, the coupling to disorder increases, and pronounced effects are expected. Disorder-driven localization and the related enhancement of the Coulomb interaction inherently compete with the attractive interaction in superconducting metals,[3,4] described by the electron-phonon spectral density $\alpha^2 F(\omega)$.[5] This competition reduces the transition temperature. Of particular interest are two-dimensional (2D) superconductors in which the degree of disorder can be adjusted by varying the appropriate parameters. In an ideal 2D system, the relevant parameter is normally considered to be the sheet resistance, $R_\square$. The sheet resistance is determined by two factors: the (possibly thickness dependent) conductivity σ and the film thickness d.

Amorphous MoGe (α-MoGe) thin films are thought to be a model system for studying the interplay between superconductivity and disorder. Several transport experiments have revealed a sharp reduction in the superconducting transition temperature T_c with increasing $R_\square$, even in the weakly localized regime[6–9] with a concomitant reduction in superfluid density.[10,11] The suppression of T_c has been attributed to localization and an increase in the Coulomb interaction.[3] In this paper, we explore the T_c suppression in α-MoGe thin films with different thicknesses via temperature-dependent far-infrared transmittance and reflectance. A strong suppression of T_c with increasing $R_\square$ is observed. The superconduct-

ing energy gap is also reduced, but the normal-state conductivity and the ratio of gap energy to transition temperature, both of which could be dependent on the disorder-driven Coulomb interaction, are not affected at all.

II. SAMPLES AND METHODS

Our films were prepared by comagnetron sputtering from elemental targets onto rapidly rotating (3 revolution/sec or 0.1 nm deposited/revolution) single-crystal r-cut ($10\bar{1}2$) sapphire substrates (1 mm thick). A 7.5 nm α-Ge underlayer was first laid down on the substrates to ensure smoothness of the subsequently deposited MoGe films. For films prepared in similar fashion, no sign of crystalline inclusions were observed by x-ray and transmission electron microscopy. This procedure is known to yield uniform and homogeneous amorphous films of near ideal stoichiometry.[6,7] A thickness monitor gave the film thickness; the remaining parameters of our films, in Table I, were all determined from optical measurements, described below.

Far-infrared measurements were performed at beamlines U10A and U12IR of the National Synchrotron Light Source

TABLE I. Parameters for MoGe films.

Film	d (nm)	T_c (K)	$R_\square$ (Ω)	$2\Delta_0$ (cm^{-1})	$2\Delta_0/kT_c$
A	4.3	<1.8	505		
B	8.3	4.5	260	12	3.7
C	16.5	6.1	131	16	3.9
D	33	6.9	69	18	3.8

at Brookhaven National Laboratory. U12IR, equipped with a Sciencetech SPS200 Martin-Puplett interferometer, was used for frequencies between 5 and 50 cm^{-1}. A Bruker IFS-66v/S rapid scan Fourier-transform interferometer at U10A was used over 20–100 cm^{-1}. A bolometer operating at 1.7 K provided excellent sensitivity; its window is responsible for the high-frequency cutoff of 100 cm^{-1}. The films were in an Oxford Instruments Optistat bath cryostat, which enabled sample temperatures of 1.7–20 K. Transmittance $T(\omega)$ and reflectance $R(\omega)$ of four films were taken at various temperatures below T_c. The normal-state transmittance and reflectance were taken at 10 K.

III. THIN-FILM OPTICS

For a metal film of thickness $d \ll \lambda$, the wavelength of the far-infrared radiation, and $d \ll \{\delta, \lambda_L\}$ the skin depth (normal state) or penetration depth (superconducting state), the transmittance across the film into the substrate and the "single-bounce" reflectance (i.e., reflectance with no contribution by the second surface) from the film are both determined by the film's complex conductivity $\sigma = \sigma_1 + i\sigma_2$ according to[12,13]

$$T_f = \frac{4n}{(Z_0\sigma_1 d + n + 1)^2 + (Z_0\sigma_2 d)^2},$$ (1)

$$R_f = \frac{(Z_0\sigma_1 d + n - 1)^2 + (Z_0\sigma_2 d)^2}{(Z_0\sigma_1 d + n + 1)^2 + (Z_0\sigma_2 d)^2},$$ (2)

where n is the refractive index of the substrate and Z_0 is the impedance of free space ($4\pi/c$ in cgs and 377 Ω in mks). Although Eqs. (1) and (2) give the essential physics of a thin film on a thick substrate, the externally measured transmittance and reflectance are influenced by multiple internal reflections within the substrate. In our case the substrate is sufficiently thick and the spectral resolution sufficiently low that these reflections can be taken as incoherent so that

$$T = T_f \frac{(1 - R_u)e^{-\alpha x}}{1 - R_u R_f' e^{-2\alpha x}},$$ (3)

$$R = R_f + \frac{T_f^2 R_u e^{-2\alpha x}}{1 - R_u R_f' e^{-2\alpha x}},$$ (4)

where the substrate has thickness x and absorption coefficient α. The single-bounce reflectance of the uncoated substrate surface is $R_u = [(1-n)^2 + \kappa^2]/[(1+n)^2 + \kappa^2] \approx [(1-n)/(1+n)]^2$. (The approximation holds when $\kappa = c\alpha/2\omega \ll n$, as is the case for our weakly absorbing sapphire substrate.) Finally, R_f' is the substrate-incident single-bounce reflection of the film,

$$R_f' = \frac{(Z_0\sigma_1 d - n + 1)^2 + (Z_0\sigma_2 d)^2}{(Z_0\sigma_1 d + n + 1)^2 + (Z_0\sigma_2 d)^2}.$$ (5)

Note that the external transmittance T is independent of the direction of travel of the infrared beam (because the transmittance of the uncoated surface is $1 - R_u$), whereas the external reflectance R differs depending on whether the film is the first (our case) or second surface.
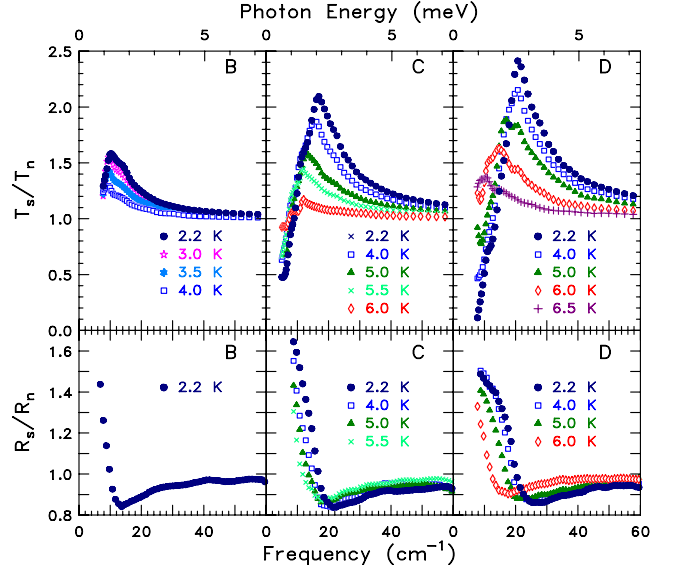

FIG. 1. (Color online) Measured transmittance and reflectance ratios of three MoGe films at several temperatures.

Measurements of T and R at each frequency determine σ_1 and σ_2. Beginning with the pioneering work of Palmer and Tinkham,[12] this approach has been used from time to time[13,14] to obtain the optical properties of superconducting thin films. The inversion process also requires knowledge of the refractive index and absorption coefficient of the substrate; we used $n = 3.05$ for r-cut sapphire and $\alpha = 0$, confirmed by measurements of uncoated substrates. Because of the asymmetry in how σ_1 and σ_2 appear in Eqs. (1) and (2), the method gives more accuracy and better signal to noise in σ_1.

As mentioned above, each of our samples had a 7.5 nm α-Ge buffer layer between the sapphire substrate and the MoGe film. Within the thin-film approximation used here, this layer adds a parallel conductance to the metal film of $\sigma_{buff}d_{buff} = -i\omega(\epsilon - 1)d_{buff}/4\pi$ with ϵ as the dielectric constant of the α-Ge. Taking[15] $\epsilon = 15.7$ (real), this contribution reduces the value of σ_2 at 50 cm^{-1} by 11 Ω^{-1} cm^{-1} in the thinnest film and by smaller amounts at lower frequencies or in thicker films. Because our films have $\sigma_N \sim 4400$ Ω^{-1} cm^{-1} (see below), we have neglected this small correction to our conductivities.

We used the broadband far-infrared transmittance to determine the transition temperature. The normal-state transmission is temperature independent (on account of the dominant residual scattering). When, as the sample temperature is decreased slowly, superconductivity occurs, the broadband transmission increases. We call T_c that temperature at which a measurable transmission increase first occurs. Finally, the normal-state infrared transmission, via Eqs. (1) and (3), gives $R_\square = 1/\sigma_n d$. [The frequency-independent transmission tells us that the normal state $\sigma_1(\omega) = \text{const} \gg \sigma_2$.]

IV. TRANSMITTANCE AND REFLECTANCE

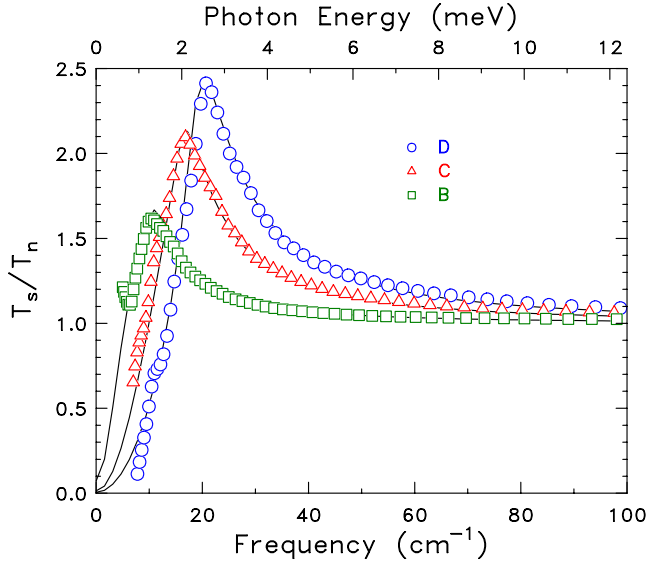Figure 1 shows the superconducting/normal transmission

FIG. 2. (Color online) T_s/T_n measured at 2.2 K (points) for the three films compared to calculations using the Mattis-Bardeen expressions for the far-infrared conductivity of a superconductor (lines).

ratio (T_s/T_n) and the reflectance ratio (R_s/R_n) at several temperatures for three films; the thinnest film did not superconduct at the lowest achievable temperature in our apparatus. The shape of the transmission curve is determined by a competition between σ_1 and σ_2 in Eq. (1). At low frequency the ratio goes to zero as $\sim\omega^2$ due to the kinetic inductance of the superfluid, which yields $\sigma_{2s}\sim1/\omega$ while at the same time $\sigma_{1s}\sim0$. The frequency of the maximum of T_s/T_n occurs very close to the superconducting gap frequency $\omega_g=2\Delta/\hbar$ because σ_{1s} rises toward the normal-state value above the gap as σ_{2s} is becoming small. There is a corresponding minimum in the reflectance. At high frequencies $T_s/T_n=1$ and $R_s/R_n=1$.

The data in Fig. 1 clearly show that the gap shrinks as temperature increases toward T_c. At a given reduced temperature T/T_c, the gap shifts to lower energy as the film becomes thinner (increasing $R_\square$). We used the dirty-limit Mattis-Bardeen[16] theory for the optical conductivity of a dirty-limit superconductor to fit the normalized transmittance T_s/T_n and reflectance R_s/R_n of our samples. Figure 2 shows the fit to the T_s/T_n ratio measured at 2.2 K for the three films that were superconducting at that temperature. The fits used Δ_0 and the normal state $R_\square$ as the two fitting parameters and assumed a BCS temperature dependence for the superconducting gap. The fits are good, consistent with the signal-to-noise ratio in the data, which deteriorates at the lowest frequencies. They find that $2\Delta_0/k_BT_c=3.8\pm0.1$, slightly higher than the BCS weak-coupling limit of 3.5. Changes in $2\Delta_0/k_BT_c$ with thickness are much smaller than the T_c reduction and not monotonic (see Table I). Fits to different temperatures and to R_s/R_n were also good.

V. OPTICAL CONDUCTIVITY

Figure 3 shows the 2.2 K results for the real and imaginary parts of the optical conductivity, $\sigma_1(\omega)$ and $\sigma_2(\omega)$, for
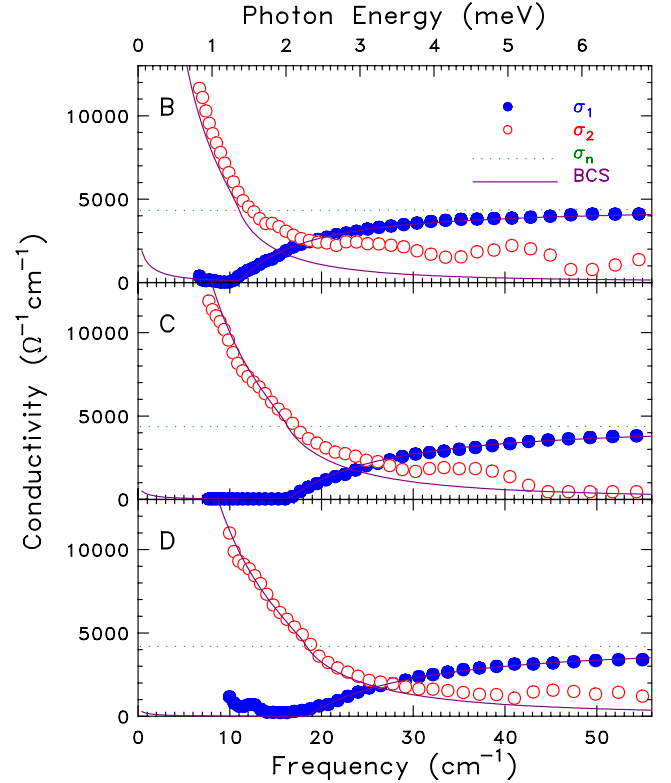

FIG. 3. (Color online) Real (filled circles) and imaginary (open circles) parts of the optical conductivity for three α-MoGe thin films. The data are taken at 2.2 K. The Mattis-Bardeen conductivity is also shown.

each film. The Mattis-Bardeen conductivities are also shown. The gap of 2Δ in the absorption spectrum is evident. All three films have approximately the same normal-state conductivity, $\sigma_N\sim4400$ Ω^{-1} cm^{-1}, obtained from transmittance measurement of film in the normal state; the superconducting-state $\sigma_1(\omega)$ approaches this value at high frequencies. Values in this range are found in transport measurements,[6,7] with the dc $R_\square$ also scaling as $1/d$. We conclude that the normal-state conductivity (or resistivity) is independent of the thickness of the film.

VI. BCS-ELIASHBERG ANALYSIS

Because the data are clearly in the dirty limit, the fitting with Mattis-Bardeen expressions is quite adequate for obtaining the value of Δ_0. In order to elucidate further features of the data, discuss changes in T_c, and make predictions, we will now move to more sophisticated calculations using BCS-Eliashberg theory. Figure 4 shows the results for the real and imaginary parts of the optical conductivity, $\sigma_1(\omega)$ and $\sigma_2(\omega)$, for film C. The lines are results of numerical calculations for the conductivity based on the Eliashberg equations and the Kubo formula for the current-current correlation function.[17] The electron-phonon spectral function was taken from that obtained through inversion of tunneling data on amorphous Mo (Ref. 18) and its mass enhancement parameter λ is fixed at 0.9. The Coulomb repulsion μ^* was adjusted to obtain the measured value of T_c. Other param-
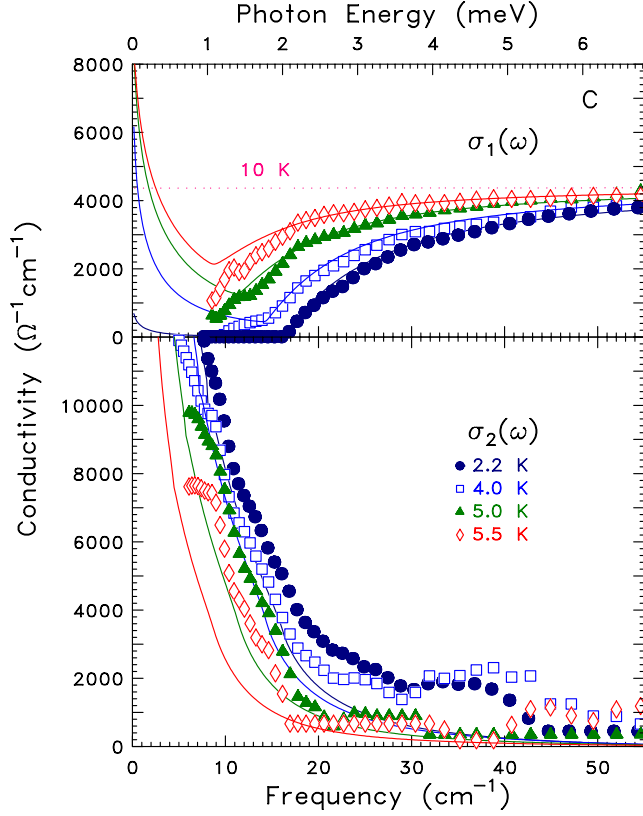
FIG. 4. (Color online) $\sigma_1(\omega)$ and $\sigma_2(\omega)$ at various temperatures for the 16.5 nm MoGe film. The points are the data and the lines are the results of our Eliashberg calculations.

eters are the impurity scattering rate $1/\tau^{imp}=3.5$ eV and the plasma energy $\Omega_p=10.7$ eV. We will see later how these were obtained from the conductivity data itself. The agreement with the data for σ_1 is best at the lowest temperature considered, with small deviations for T near T_c. This is true for all three films. The theory for σ_2 agrees with the $\sim1/\omega$ low-frequency behavior but tends to be below the experiment, especially at higher frequencies. The fit is less good with increasing T, although the qualitative behavior is given correctly.

As changing the thickness of the sample could change both μ^* and the electron-phonon interaction, there is some choice in fitting the data with Eliashberg theory. In Fig. 5, we show results for T_c and the gap ratio as a function of μ^* for three values of λ. For fixed λ, the points on the T_c curve are from the experimental data for the MoGe films, illustrating the μ^* needed to obtain the T_c. With μ^* and λ now fixed, the experimental points for the gap ratio can be compared to the prediction and there is good agreement. It is clear from this figure that keeping the ratio at 3.8 can be achieved through a change in μ^* as suggested in Refs. 1–4 but one cannot rule out additional small changes in λ. In fact, Höhn and Mitrović[19] in their Eliashberg analysis of tunneling data on disordered Pb films found evidence for a change in both these parameters with changing $E_F\tau^{imp}$, where E_F is the Fermi energy. Here such differences will not matter as we are in an impurity-dominated regime and the optics is not sensitive to the μ^* or λ value as we will explain. A λ of order 1 is
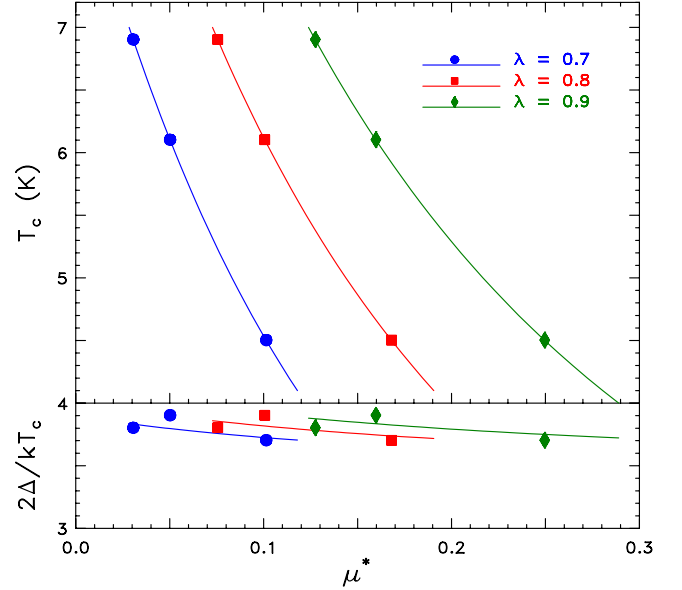

FIG. 5. (Color online) Dependence of T_c and $2\Delta/k_BT_c$ on Coulomb repulsion μ^* for three values of electron-phonon mass enhancement λ.

needed, however, to get the measured value of the gap to T_c. For definiteness, we only change μ^* leaving $\alpha^2F(\omega)$ fixed.

To proceed with the analysis, we introduce the optical self-energy $\Sigma^{op}(T,\omega)$ and use the extended Drude model, where the conductivity is written as $\sigma(T,\omega)=(i\Omega_p^2/4\pi)/[\omega-2\Sigma^{op}(T,\omega)]$. The real part of Σ^{op} gives the optical mass renormalization $\lambda^{op}(T,\omega)$ with $\omega\lambda^{op}(T,\omega)=-2\Sigma_1^{op}(T,\omega)$ and its imaginary part is related to the optical scattering rate according to $1/\tau^{op}(T,\omega)=-2\Sigma_2^{op}(T,\omega)$. The extended Drude model has been used extensively in the literature for both the normal and superconducting states. In particular, for the superconducting state some examples may be found in Refs. 17 and 20–26. Indeed, the usefulness of the extended Drude model for both situations recently has been demonstrated,[27] where it has been thoroughly examined and tested against high quality data for Pb. Transforming the optical conductivity via the extended Drude model is much like the use of Fourier transforms; some features of the information embedded in the original quantity are brought out more clearly in the transformed one. In the case of the extended Drude model, the optical scattering rate clearly separates the elastic and inelastic contributions in the normal state, while in the superconducting state it shows the coherence peak which is related to that formed in the tunneling density of states. The optical mass at zero frequency gives the quasiparticle mass renormalization in the normal state and the inverse of the superfluid density in the superconducting state. The peak in both the optical scattering rate and mass renormalization in the superconducting state marks the energy scale 2Δ and can only exist in the presence of impurity scattering.

For MoGe, these quantities are shown in Fig. 6 for the thickest and thinnest superconducting samples at $T=2.2$ K. To obtain $1/\tau^{op}$, we had to use an impurity scattering rate of 3.5 eV. For $v_F\sim1.5\times10^8$ cm/s, this rate corresponds to a mean free path of ~0.3 nm. This value, while small, is con-
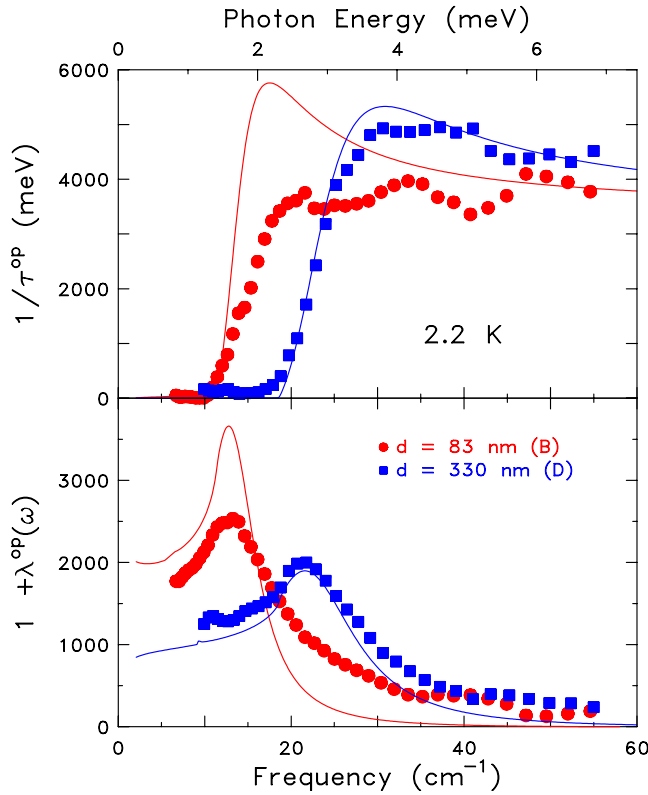
FIG. 6. (Color online) Optical scattering rate $1/\tau^{op}(\omega)$ and mass renormalization $1+\lambda^{op}(\omega)$ for the thickest and thinnest superconducting films. Points are data and lines are Eliashberg calculations for the extreme dirty limit.
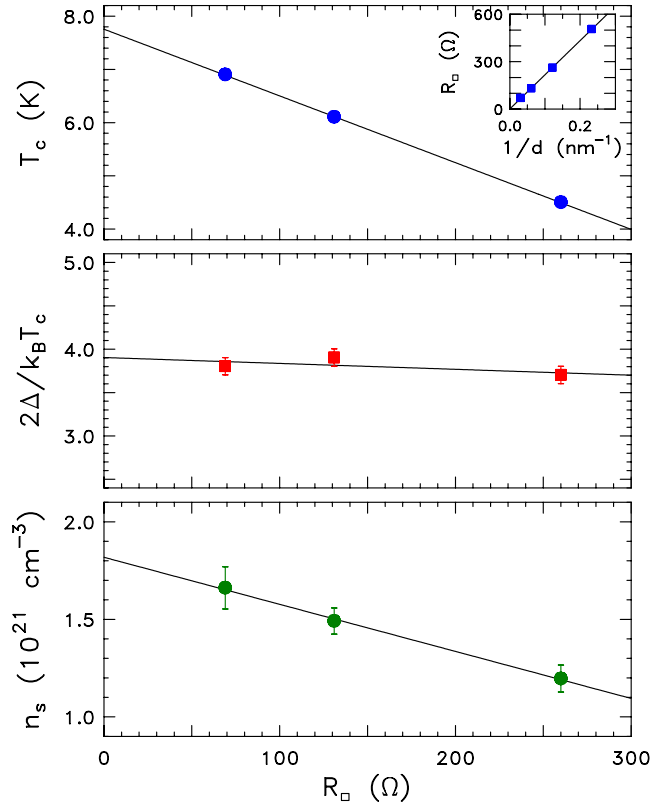

FIG. 7. (Color online) The dependence of T_c, gap ratio, and superfluid density n_s on $R_\square$. The inset in the upper panel shows the linear dependence of $R_\square$ on the inverse of the film thickness d. Linear fits to all quantities are shown.

sistent with other estimates and is much less than the thickness of the films.[6] Hence surface scattering is not important, $R_\square \propto 1/d$, and the normal-state conductivity does not depend on sheet resistance.

VII. DISCUSSION AND CONCLUSIONS

It is important to understand that the peaks in $1/\tau^{op}(\omega)$ are the optical equivalent of density-of-states coherence peaks. The calculation for the thickest film fits the data well but for the thinner film the peak is very much attenuated, perhaps indicating an effect outside standard Eliashberg theory. In their tunneling study of the metal-insulator transition in aluminum films, Dynes *et al.*[28] found a similar effect, namely, a broadening of the density-of-states coherence peak with increased sheet resistance. The lower panel of Fig. 6 gives the optical effective mass in the superconducting state. We note the large peak at $2\Delta_0$ in $1+\lambda^{op}$, predicted by theory and seen in the data. This peak is related through Kramers-Kronig transformation to the sharp rise in $1/\tau^{op}(\omega)$ at this same frequency. For both samples as $\omega \to 0$, the effective mass is very large, of the order of 1000, comparable to heavy fermion masses, although the origin of the large mass is quite different. Here, these values reflect directly the large impurity scattering and are related to the decrease in superfluid density with decreasing τ^{imp}. The physical meaning of this optical mass is that it is to replace the bare mass in the clean-

limit formula for the London penetration depth if it is retained when impurities are included.

In an Eliashberg superconductor, the superfluid density (n_s) at $T=0$ in the clean-limit case is given by $n_s^{clean}(T=0) = n/(1+\lambda)$, where n is the electron density. In the dirty limit where $1/[2\Delta_0\tau^{imp}(1+\lambda)] \gg 1$, it is instead given by $n_s^{dirty}(T=0) = n\pi\Delta_0\tau^{imp}$ with λ dropping out.[17] For fixed n, this gives immediately[29,30] a relation between the superfluid density n_s, T_c, and σ_n.

Figure 7 shows the dependence of various superconducting-state quantities on the sheet resistance, $R_\square$. The top panel shows that T_c decreases almost a factor of 2 over the range of sheet resistances studied here. The inset indicates that $R_\square$ increases linearly with $1/d$, with d as the film thickness. Hence, the normal-state conductivity is not dependent on $R_\square$. The middle panel shows the gap ratio $2\Delta(0)/k_BT_c$ vs $R_\square$. The gap ratio is essentially independent of $R_\square$. The bottom panel shows the superfluid density n_s obtained from $n_s = m\omega\sigma_2/e^2$, with m as the free-electron mass and e as the electronic charge. n_s is a frequency-dependent quantity but nearly constant over frequency on account of the $1/\omega$ behavior of σ_2; we report the average over $10-30$ cm^{-1}. The superfluid density n_s depends strongly on $R_\square$. This behavior is also seen by mutual inductance measurements[10,11] of the low-frequency kinetic inductance of MoGe and as well in similar measurements of dirty-limit Nb films.[31]

A comparison of the slopes of the T_c and n_s functions shows that T_c is nearly proportional to the superfluid density.

This behavior is reminiscent of the cuprate superconductors, where a linear relation between n_s and T_c is well established and is thought to be causal.[29] However, in the dirty-limit case, as in α-MoGe, the relation is trivial: a reduction in T_c (from whatever cause) leads immediately to a decrease in n_s. The explanation goes as follows. The $1/\omega$ behavior of $\sigma_2(\omega)$ is a direct consequence (via the Kramers-Kronig relations) of the delta function at the origin in $\sigma_1(\omega)$ (the infinite dc conductivity of the superconductor) and the weight of this delta function is proportional to n_s. In turn, the Ferrell-Glover-Tinkham sum rule[32] relates the strength of the delta function to the "missing area" in $\sigma_1(\omega)$ caused by the opening of the superconducting gap. (See the upper panel of Fig. 4; the missing area would be the area between the dotted line and the superconducting-state conductivity.) Thus, the missing area, A, can be written as $A = \sigma_n 2\Delta C \approx \sigma_n T_c 3.8 k_B C$, where C is some constant that describes the line shape of the gap absorption. Because the normal-state conductivity is the same for each sample, the missing area, and hence n_s increases with T_c.

In summary, the observed strong suppression of T_c while at the same time the gap ratio $2\Delta_0/kT_c$ remains at 3.8, can be understood as due to a small decrease in λ and/or an increase in μ^*. BCS-Eliashberg theory gives an excellent description of our finding even though the elastic-scattering rate is very large (3.5 eV) and associated mean free path is extremely short (a few angstroms). This behavior is a striking confirmation of Anderson's theorem, which states that impurity scattering drops out of the gap ratio in an isotropic *s*-wave superconductor.[17] Nevertheless, an important discrepancy is found in the thinner film where the predicted coherence peak in the optical scattering rate is found to be strongly suppressed. This suppression is unlikely to be explained through the ideas of localization because we observed no change in the normal-state conductivity. Consequently, this observation provides a challenge to the theoretical community.

[1] P. W. Anderson, E. Abrahams, and T. V. Ramakrishnan, Phys. Rev. Lett. **43**, 718 (1979).

[2] B. L. Altshuler, A. G. Aronov, and P. A. Lee, Phys. Rev. Lett. **44**, 1288 (1980).

[3] S. Maekawa and H. Fukuyama, J. Phys. Soc. Jpn. **51**, 1380 (1982).

[4] P. W. Anderson, K. A. Muttalib, and T. V. Ramakrishnan, Phys. Rev. B **28**, 117 (1983).

[5] J. P. Carbotte, Rev. Mod. Phys. **62**, 1027 (1990).

[6] J. M. Graybeal and M. R. Beasley, Phys. Rev. B **29**, 4167 (1984).

[7] J. M. Graybeal, Physica B (Amsterdam) **135**, 113 (1985).

[8] M. Strongin, R. S. Thompson, O. F. Kammerer, and J. F. Crow, Phys. Rev. B **1**, 1078 (1970).

[9] H. Raffy, R. B. Laibowitz, P. Chaudhari, and S. Maekawa, Phys. Rev. B **28**, 6607 (1983).

[10] S. J. Turneaure, T. R. Lemberger, and J. M. Graybeal, Phys. Rev. Lett. **84**, 987 (2000).

[11] S. J. Turneaure, T. R. Lemberger, and J. M. Graybeal, Phys. Rev. B **63**, 174505 (2001).

[12] L. H. Palmer and M. Tinkham, Phys. Rev. **165**, 588 (1968).

[13] F. Gao, G. L. Carr, C. D. Porter, D. B. Tanner, G. P. Williams, C. J. Hirschmugl, B. Dutta, X. D. Wu, and S. Etemad, Phys. Rev. B **54**, 700 (1996).

[14] D. R. Karecki, G. L. Carr, S. Perkowitz, D. U. Gubser, and S. A. Wolf, Phys. Rev. B **27**, 5460 (1983).

[15] S. H. Wemple, Phys. Rev. B **7**, 3767 (1973).

[16] D. C. Mattis and J. Bardeen, Phys. Rev. **111**, 412 (1958).

[17] F. Marsiglio and J. P. Carbotte, in *Physics of Conventional and High T_c Superconductors*, edited by H. H. Bennemann and J. B. Ketterson (Springer-Verlag, Berlin, 2002), Vol. 1, p. 233.

[18] D. B. Kimhi and T. H. Geballe, Phys. Rev. Lett. **45**, 1039 (1980).

[19] T. Höhn and B. Mitrović, Z. Phys. B: Condens. Matter **93**, 173 (1994).

[20] D. N. Basov, R. Liang, B. Dabrowski, D. A. Bonn, W. N. Hardy, and T. Timusk, Phys. Rev. Lett. **77**, 4090 (1996).

[21] A. V. Puchkov, D. N. Basov, and T. Timusk, J. Phys.: Condens. Matter **8**, 10049 (1996).

[22] J. P. Carbotte, E. Schachinger, and D. N. Basov, Nature (London) **401**, 354 (1999).

[23] J. P. Carbotte, E. Schachinger, and J. Hwang, Phys. Rev. B **71**, 054506 (2005).

[24] J. Hwang, T. Timusk, and G. D. Gu, J. Phys.: Condens. Matter **19**, 125208 (2007).

[25] D. N. Basov, E. J. Singley, and S. V. Dordevic, Phys. Rev. B **65**, 054516 (2002).

[26] A. V. Chubukov, Ar. Abanov, and D. N. Basov, Phys. Rev. B **68**, 024504 (2003).

[27] T. Mori, E. J. Nicol, S. Shiizuka, K. Kuniyasu, T. Nojima, N. Toyota, and J. P. Carbotte, Phys. Rev. B **77**, 174515 (2008).

[28] R. C. Dynes, J. P. Garno, G. B. Hertel, and T. P. Orlando, Phys. Rev. Lett. **53**, 2437 (1984).

[29] Y. J. Uemura, L. P. Le, G. M. Luke, B. J. Sternlieb, W. D. Wu, J. H. Brewer, T. M. Riseman, C. L. Seaman, M. B. Maple, M. Ishikawa, D. G. Hinks, J. D. Jorgensen, G. Saito, and H. Yamochi, Phys. Rev. Lett. **66**, 2665 (1991).

[30] C. C. Homes, S. V. Dordevic, M. Strongin, D. A. Bonn, Ruixing Liang, W. N. Hardy, Seiki Komiya, Yoichi Ando, G. Yu, N. Kaneko, X. Zhao, M. Greven, D. N. Basov, and T. Timusk, Nature (London) **430**, 539 (2004).

[31] T. R. Lemberger, I. Hetel, J. W. Knepper, and F. Y. Yang, Phys. Rev. B **76**, 094515 (2007).

[32] R. A. Ferrell and R. E. Glover, Phys. Rev. **109**, 1398 (1958); M. Tinkham and R. A. Ferrell, Phys. Rev. Lett. **2**, 331 (1959).